# Nano-Modified Fly Ash Concrete: A Repair Option for Concrete Pavements

by A. Ghazy, M. T. Bassuoni, and A. Shalaby

*Efficient repair of concrete pavements typically requires a rapid-setting material to accelerate opening the road to traffic. While numerous high-early-strength cementitious repair materials are commercially available, many of them are vulnerable to premature deterioration. On the other hand, despite its improved long-term performance, concrete incorporating fly ash is rarely used as a repair material due to the delay in setting time, strength gain, and microstructural development at early ages. Nevertheless, these performance limitations can be mitigated by incorporation of nanoparticles (for example, nanosilica) in fly ash concrete. In this study, an effort was made to develop nano-modified fly ash concrete as a repair material for concrete pavements. The performance of the newly developed mixtures was compared to that of two commercial cementitious products. The results indicate that the nano-modified fly ash concrete has balanced performance in terms of hardening time, strength development, bonding with substrate concrete, and resistance to infiltration of fluids and salt-frost scaling.*

Keywords: durability; early age; fly ash; nanosilica; repair.

## INTRODUCTION

Premature failure of repairs in concrete pavements and bridge decks is frequently observed, resulting in significant life-cycle, economic, and social losses.[1,2] Efficient repair of concrete pavements typically requires a rapid-setting material that can be placed and hardened within a relatively short period of time for quick opening to traffic. While numerous high-early-strength cementitious repair materials are commercially available, many of these materials are vulnerable to cracking, poor bonding, and premature deterioration, for example, due to incompatibility with the existing concrete pavement.[2,3] In addition, some studies have shown concerns of using high-early-strength concrete in repair applications for pavements.[4] These materials can lead to stress concentrations because of their susceptibility to thermal gradients and autogenous shrinkage, resulting in high levels of microcracking and, in turn, durability issues.

Extensive research on the use of supplementary cementitious materials (SCMs) such as fly ash showed that incorporation of Class F fly ash generally improves the long-term performance and durability of concrete.[5-7] Despite the benefits of fly ash concrete, practical limitations remain unresolved in field applications. The delay in setting time, strength gain, and microstructural development at early ages of fly ash concrete are considered to be the major issues, which deter its wider acceptance as a repair material.[6-8] Also, a number of laboratory studies have indicated inferior scaling resistance of concrete containing dosages of fly ash in excess of 25 to 30% of the binder when subjected to cycles of freezing and thawing in the presence of deicing chemicals.[6,7]

Recently, nanomaterials have been progressively applied in the field of concrete research, attracting considerable scientific interest due to the new potential uses of nanometer-sized particles in cementitious binders. Concrete with superior properties can be produced by incorporating nanoparticles with fly ash.[8-11] As a result of their ultrafine nature (size scale of 1-100 billionth of a meter), nanoparticles can vigorously speed up the kinetics of cement hydration in concrete.[8-11] Hence, the delay in setting time, strength gain, and microstructural development of fly ash concrete may be mitigated.

## RESEARCH SIGNIFICANCE

Carefully balancing the early-age and long-term performance of cement-based repair materials remains a challenging task, which warrants further investigation. In comparison to two cementitious products specified by transportation agencies in Manitoba for partial-depth repair of concrete pavements, an effort was made in the present study to develop nano-modified fly ash concrete as a repair material for concrete pavements to achieve balanced performance in terms of hardening time, strength development, bonding with substrate concrete, and durability to infiltration of fluids and salt-frost scaling.

## EXPERIMENTAL PROCEDURE

### Materials

General use (GU) portland cement and fly ash (Class F), which meet the requirements of the CAN/CSA-A3001[12] standard, were used as the main components of the binder. Their chemical and physical properties are shown in Table 1. In addition, a commercial nano-silica sol (50% solid content of $SiO_2$ dispersed in an aqueous solution [Table 1]) was incorporated in all binders. Six concrete mixtures were prepared and a non-chloride accelerator, complying with ASTM C494/C494M[13] Type E, was used in three mixtures to accelerate the setting time. Locally available coarse aggregate (natural gravel with a maximum size of 9.5 mm [0.375 in.]) and fine aggregate (well-graded river sand with a fineness modulus of 2.9) were used. The specific gravity and absorption were 2.65 and 2%, respectively, for gravel, and 2.53 and 1.5%, respectively, for sand. A high-range water-reducing

## Table 1—Properties of GU cement, fly ash, and nanosilica

|  | Cement | Fly ash | Nanosilica |
|---|---|---|---|
| $SiO_2$,% | 19.21 | 55.20 | 99.17 |
| $Al_2O_3$,% | 5.01 | 23.13 | 0.38 |
| $Fe_2O_3$,% | 2.33 | 3.62 | 0.02 |
| CaO,% | 63.22 | 10.81 | — |
| MgO,% | 3.31 | 1.11 | 0.21 |
| $SO_3$,% | 3.01 | 0.22 | — |
| $Na_2O_{eq}$,% | 0.12 | 3.21 | 0.20 |
| Specific gravity | 3.15 | 2.12 | 1.40 |
| Mean particle size, μm (in.) | 13.15 $(8.45 \times 10^{-6})$ | 16.56 $(6.52 \times 10^{-6})$ | $35 \times 10^{-3}$ $(1.38 \times 10^{-6})$ |
| Fineness, $m^2$/kg ($ft^2$/lb) | 390 $(1.90 \times 10^3)$* | 290 $(1.41 \times 10^3)$* | 80,000 $(0.39 \times 10^6)$† |
| Viscosity, Cp (ft·s/lb) | — | — | 8 $(0.537 \times 10^{-2})$ |
| pH | — | — | 9.5 |

*Blaine fineness.

†Fineness was determined by titration with sodium hydroxide.

## Table 2–Composition and properties of commercial products according to manufacturers' datasheets

|  | A | B |
|---|---|---|
| Composition, % by mass | | |
| Hydraulic cement | ✓* | 7 to 13 |
| Silica sand, crystalline | ✓ | >60 |
| Titanium dioxide | ✓ | 0.1 to 1 |
| Borax | ✓ | 1 to 5 |
| Physical properties | | |
| Specific gravity | 2.7 | 2.75 |
| Water content, L/22.7 kg (gal/50 lb) | 2.1 to 2.8 (0.56 to 0.75) | 1.6 to 1.8 (0.42 to 0.47) |
| Mixing time, min | 4 to 5 | 4 |
| Extension† | 50% | 50% |
| Curing procedures | Wet cure surface with water and polyethylene sheets at least 1 day, or use a curing compound | |

*Range is not specified in datasheet.

†Coarse aggregate extension by mass of repair material per bag, 22.7 kg (50 lb).

admixture (HRWRA) based on polycarboxylic acid and complying with ASTM C494/C494M[13] Type F was added to maintain a slump range of 50 to 100 mm (1.97 to 3.94 in.). In addition, an air-entraining admixture was used to provide a fresh air content of 6 ± 1%. For comparison purposes, two commercial cementitious repair materials were evaluated. These products are approved and used in the province of Manitoba based on the premise that they achieve early-age performance and adequate service life. Table 2 shows their composition and physical properties according to each manufacturer's datasheet.

## Procedures

The formulations of the nano-modified fly ash concrete stem from a compatibility perspective between repair and parent concrete; thus, all the repair mixtures comprised fly ash comparable to concrete pavements in Manitoba, in which 15% fly ash is typically used. Three normal-setting concrete mixtures (designated as N) were prepared with GU cement and variable dosages of fly ash (15%, 22.5%, and 30% replacement by mass of the base binder (385 kg/m³ [24 lb/ft³]) comprising GU cement and fly ash); nanosilica was added to the mixtures at a single dosage of 6% by mass of the base binder (that is, a solid content of 23 kg/m³ [1.44 lb/ft³]). In addition, three corresponding rapid-setting concrete mixtures (designated as R) were produced with an accelerating admixture. For all mixtures, the total cementitious materials (ternary binder: GU cement, fly ash, and nanosilica) content and water cementitious materials ratio (w/cm) were kept constant at 408 kg/m³ (25 lb/ft³) and 0.38, respectively.

Constituent materials were mixed in a concrete mixer with a speed of 60 rpm. To attain homogenous dispersion of components, a specific sequence of mixing was adopted based on experimental trials. First, approximately 15% of the mixing water was added to the aggregate while mixing

for 30 seconds. The cement and fly ash were then added to the aggregate and mixed together for 60 seconds. The nanosilica and the admixtures (air-entraining admixture, HRWRA, and accelerator) were added to the remaining water while stirring vigorously for 45 seconds to obtain a liquid phase containing well-dispersed nanoparticles and admixtures. Finally, the liquid phase was added to the mixture and mixing continued for 2 minutes. After mixing and casting the concrete, a vibrating table was used to ensure good compaction of specimens. Polyethylene sheets were used to cover the surface of specimens for 24 hours. The specimens were then demolded and cured in a standard curing room (maintained at a temperature of 22 ± 2°C [72 ± 3.6°F] and a relative humidity of more than 95%) until testing. The proportions of the nano-modified mixtures are shown in Table 3. For the commercial products, the manufacturers' recommendations were carefully followed in the proportioning, mixing, casting, and curing procedures (Table 2).

## Testing methods

To determine the setting time, the mortar fraction of each mixture (portion passing sieve No. 4 [4.75 mm (0.19 in.)]) was placed in a container at room temperature as specified by ASTM C403.[14] At regular time intervals, the penetration resistance was determined by standard needles. In addition, paste samples with identical proportions to the paste fraction in the concrete mixtures (Table 3) were prepared to measure the heat released from the hydration reactions by an isothermal calorimeter kept at 23°C (73°F) following the general guidelines of ASTM C1679.[15] The rate of heat generated was monitored and recorded every minute continuously for 100 hours, and it was normalized by the mass of the sample. Also, the cumulative heat released was determined.

For each mixture, triplicate 100 x 200 mm (4 x 8 in.) concrete cylinders were prepared for the compressive

**Table 3—Proportions of mixtures per cubic meter of concrete**

| Mixture ID | Cement, kg | Fly ash, kg | Nanosilica, kg | Water*, kg | Coarse aggregate, kg | Fine aggregate, kg | HRWRA, L/m$^3$ | Accelerator, L/m$^3$ |
|---|---|---|---|---|---|---|---|---|
| F15 | 327 | 58 | 0 | 147 | 858 | 858 | 0.7 | 0 |
| F30 | 269 | 116 | 0 | 147 | 850 | 850 | 0.4 | 0 |
| NF15 | 327 | 58 | 46 | 131 | 830 | 830 | 2.3 | 0 |
| NF22.5 | 298 | 87 | 46 | 131 | 830 | 830 | 2.1 | 0 |
| NF30 | 269 | 116 | 46 | 131 | 830 | 830 | 1.9 | 0 |
| RF15 | 327 | 58 | 46 | 131 | 830 | 830 | 1.8 | 6.9 |
| RF22.5 | 298 | 87 | 46 | 131 | 830 | 830 | 1.7 | 6.9 |
| RF30 | 269 | 116 | 46 | 131 | 830 | 830 | 1.5 | 6.9 |

*Adjusted amount of mixing water considering water content of nanosilica (aqueous solution with 50% solid content of SiO$_2$).

Note: 1 kg = 2.205 lb; 1 L/m$^3$ = 7.48 × 10$^3$ gal/ft$^3$.

strength test according to ASTM C39[16] and splitting tensile strength test according to ASTM C496,[17] which were performed at different ages. To evaluate the bond between the repair mixtures and concrete substrate along with the resistance of the composite assembly to environmental conditioning, the pulloff test was used according to CSA A23.2-6B.[18] Concrete slabs of 300 x 400 mm (11.8 x 15.8 in.) surface area and 140 mm (5.5 in.) thickness were used as concrete substrate (350 kg [772 lb] GU cement with 15% fly ash as a binder replacement and 0.38 *w/cm*). After casting, the slabs were demolded and moist cured for 7 days in the curing room and then maintained in normal laboratory conditions. At 90 days, the top surface (finished surface) was wire brushed and cleaned; subsequently, the repair mixtures were placed on the top surface with a thickness of 80 mm (3.15 in.). After moist curing for 28 days, the slabs were partially cored to determine the pulloff strength according to CSA A23.2-6B.[18] Furthermore, the bond strength of companion slabs was evaluated after consecutive freezing-and-thawing (F/T) and wetting-and-drying (W/D) cycles. A total of 25 F/T cycles followed by 25 W/D cycles were applied. This customized procedure simulates climatic conditions of successive winter and summer seasons, which correlates to in-service conditions. For the F/T stage, ASTM C672/C672M[19] regime was applied for 25 cycles. Subsequently, the specimens were exposed to 25 W/D cycles, where each cycle consisted of ponding (3 to 5 mm [0.12 to 0.20 in.]) the surface of specimens with 4% calcium chloride solution for 16 hours at a temperature of 22 ± 2°C (73 ± 3.6°F), followed by drying at 40 ± 2°C (104 ± 3.6°F) and 40 ± 5% RH for 8 hours.

At 28 days, the resistance of the mixtures to the penetrability of aggressive ions was evaluated by the rapid chloride penetrability test (RCPT) according to ASTM C1202.[20] To avoid the electrolysis bias of this method, the penetration depth of chloride ions into concrete, which better correlates to the physical characteristics of the pore structure, was determined according to the procedure described by Bassuoni et al. in 2006.[21] After the RCPT, the specimens were axially split and sprayed with 0.1 M silver nitrate solution, which forms a white precipitate of silver chloride in approximately 15 minutes, to measure the physical penetration depth of chloride ions. The average depth of the white precipitate was determined at five different locations along the diameter of each half specimen. This depth is considered to be an indication of the ease of ingress of external fluids and, thus, the continuity of the microstructure.[21] In addition, ASTM C672/C672M[19] was conducted for all the mixtures to evaluate their resistance to surface scaling due to deicing salts (4% calcium chloride) and F/T cycles. The resistance to surface scaling was evaluated when the curing method (by a chemical compound or a standard curing room) and time (3 to 14 days) were varied. Moreover, the resistance to surface scaling was evaluated qualitatively by visual examination, and quantitatively by mass of scaled materials.

Thermal and microscopy studies were conducted to evaluate the evolution of microstructure in the concrete mixtures. The quantity of portlandite (calcium hydroxide) in the matrix was determined up to 90 days to assess the effect of nanosilica and fly ash on the hydration and pozzolanic reactions. Thermogravimetry (TG) at a heating rate of 10°C/min (18°F/min) was used for this purpose on powder samples extracted from the concrete mixtures. The content of portlandite was calculated by determining the percentage drop of an ignited mass of the TG curves at a temperature range of 400 to 450°C (752 to 842°F) and multiplying it by 4.11 (ratio of the molecular mass of portlandite to that of water). Backscattered scanning electron microscopy (BSEM) with elemental dispersive X-ray (EDX) were conducted on polished thin sections from the concrete mixtures. At 28 days, slices were cut from specimens, which were then dried and impregnated by a low-viscosity epoxy resin under vacuum pressure and polished by successive diamond surface-grinding to a thickness of 30 to 50 μm (1.18 × 10$^{-3}$ to 1.97 × 10$^{-3}$ in.). The sections were coated with carbon to enhance the conductivity for the BSEM analysis. Finally, selected tests (setting time, heat of hydration, and thermal analysis) were also done on reference fly ash concrete mixtures (without nanosilica) comprising 15% and 30% fly ash (F15 and F30) to exemplify the difference in behavior relative to the nano-modified fly ash concrete.

## EXPERIMENTAL RESULTS AND DISCUSSION
### Fresh properties and heat of hydration

Table 4 shows the properties of fresh concrete, including density, slump, and setting times (initial and final). Products A and B showed very dry consistency (zero slump) and had very short hardening times (40 to 60 minutes), as indi-

**Table 4—Density, slump, and initial and final setting times**

| Mixture ID. | A | B | F15 | F30 | NF15 | NF22.5 | NF30 | RF15 | RF22.5 | RF30 |
|---|---|---|---|---|---|---|---|---|---|---|
| Density, kg/m³ | 2312 | 2280 | 2249 | 2233 | 2224 | 2224 | 2224 | 2231 | 2231 | 2230 |
| Slump, mm | 0 | 0 | 75 | 95 | 55 | 65 | 80 | 75 | 90 | 100 |
| Initial, min | 40 | 40 | 450 | 550 | 270 | 345 | 360 | 165 | 175 | 210 |
| Final, min | 45 | 60 | 605 | 830 | 415 | 475 | 505 | 285 | 295 | 340 |

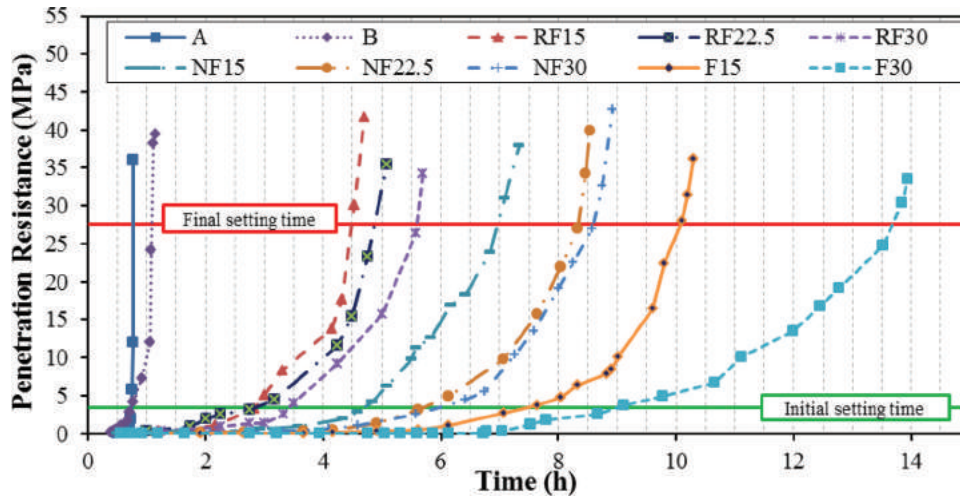Note: 1 kg/m³ = 0.0624 lb/ft³; 1 mm = 0.0394 in.



*Fig. 1—Penetration resistance versus time. (Note: 1 MPa = 145 psi.)*

cated by the acute increase of the penetration resistance curves (Fig. 1). This may imply critical placement, consolidation, and finishing, as all these procedures should be completed within 40 minutes. Also, when large patches are repaired, there will be a high potential for cold joints as repair mortars/concretes are typically mixed on site in small batches. Comparatively, the nano-modified fly ash concrete mixtures had better workability, especially the R mixtures owing to the effect of Type E (water reducer and accelerator) admixture combined with the HRWRA. Also, they had ample setting times (Fig. 1), which would allow more flexibility in the repair process, especially for large or multiple patches.

The effect of higher dosages of fly ash on retarding the setting time of concrete is well-documented,[5-7] as depicted in Fig. 1. For example, the reference concrete mixture containing 30% fly ash (F30) exhibited initial and final setting times of, respectively, 100 and 225 minutes longer than that of the reference mixture with 15% fly ash (F15). However, the setting times of the nano-modified mixtures were significantly shortened relative to the reference mixtures. For example, the initial setting times for NF15 and RF15 were 270 and 165 minutes, respectively, compared to 450 minutes for the corresponding reference mixture, F15. Also, at a higher dosage of fly ash, Mixtures NF30 and RF30 exhibited final setting times 40% and 60%, respectively, shorter than the reference mixture F30. This is ascribed to the addition of ultrafine silica particles, which accelerated the kinetics of hydration and pozzolanic reactions.[8-11] This effect was magnified with the incorporation of an accelerating admixture. For example, RF15 and RF30 exhibited final setting times of 130 and 165 minutes shorter than that of NF15 and NF30, respectively.

Isothermal calorimetry was conducted on paste samples to complement the trends observed in the setting time test. A rapid rise in the first segment of the heat flow curve may indicate initial setting (end of the dormant period) of the paste, while the peak of the curve indicates its final setting (end of acceleration stage).[22,23] For comparison purposes, the heat flow data presented herein are shown over 48 to 80 hours; however, the steady-state stage was developed up to 100 hours. The heat flow and cumulative heat released at 23°C (73°F) for the reference pastes as well as the N and R mixtures are shown in Fig. 2. It can be noted that the heat of hydration curves for the reference samples (without nanosilica) were different from that for the fly ash pastes with nanosilica. The curves for the reference cement pastes were likely dominated by hydration of tricalcium silicate ($C_3S$), similar to the hydration features observed for neat portland cement pastes[22,23]; however, the nano-modified fly ash pastes (both the N and R mixtures) were typified by a second peak (Fig. 2(b) and 2(c)) with a higher magnitude of heat flow, likely due to the accelerating effect of nanosilica on the reactions. Previous studies attributed the accelerated hydration of $C_3S$ to the higher conversion rate of the protective hydrate layer formed close to the $C_3S$ surface to a less permeable form due to the abundance of silicate ions[24] from nanosilica aggregates (agglomerates of nanosilica in the pore solution, for example due to high pH[25] or bridging of silica particles by calcium ions[26]) and reduction of calcium ions through fast pozzolanic activity (within a few hours).[9,27] This led to shortening the induction period and initial setting time of nano-modified fly ash concrete. In addition, it has been postulated that silica aggregates can accelerate the hydration of cement by
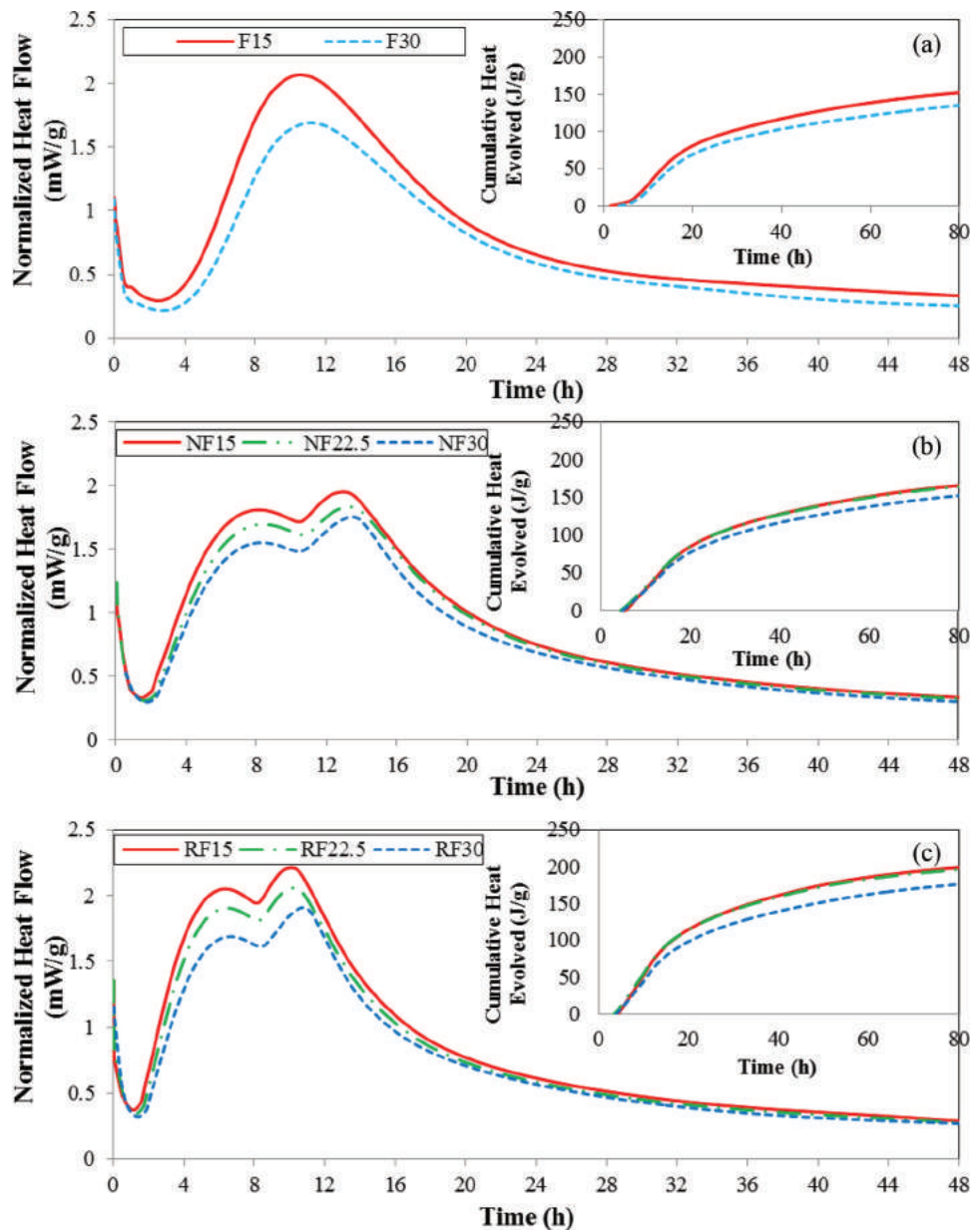
*Fig. 2—Isothermal calorimetry curves (normalized heat flow and cumulative heat released) at 23°C (73.4°F): (a) reference mixtures; (b) N mixtures; and (c) R mixtures. (Note: 1 mW/g = 1.548 BTU/(h·lb); 1 J/g = 0.43 BTU/lb.)*

creating additional surfaces for early precipitation of hydration products and, thus, reducing the final setting time.[9,11,27]

For the reference pastes, the peak of the heat flow curve was observed at 615 and 675 minutes for the reference pastes comprising 15% and 30% fly ash, respectively (Fig. 2(a)). Comparatively, the hydration of the N nano-modified fly ash pastes was significantly accelerated (Fig. 2(b)) and the length of the dormant period was markedly shortened (by approximately 120 minutes). At a dosage of 6% nanosilica, the first peaks of the hydration curves for NF15 and NF30 were obtained at, respectively, approximately 150 and 180 minutes earlier than that of the corresponding reference pastes. In addition, the total heat evolved over 80 hours was 12 to 18% higher for the N nano-modified fly ash pastes relative to the reference pastes. Again, this catalytic effect of nanosilica was magnified with the incorporation of the accelerating admixture (Fig. 2(c)). For instance, the

first peaks of the normalized heat flow curves of the RF15, RF22.5, and RF30 mixtures were obtained at, respectively, approximately 175, 155, and 130 minutes earlier than that of the corresponding N mixtures (shifted to the left), and the total cumulative heat of the R mixtures was higher (16 to 21%) than that of the N mixtures.

In compliance with the setting time trends that captured the retarding effect of the higher dosage of fly ash, it can be noted that there is a slight delay in the hydration of the mixtures containing 30% fly ash (Fig. 2(b) and 2(c)). The first hydration peaks of mixtures NF30 and RF30 were shifted to the right by approximately 30 and 15 minutes, respectively, relative to that of mixtures NF15 and RF15. Correspondingly, at 80 hours, the total cumulative heat released from the pastes comprising 30% fly ash was lower than that from pastes with 15% fly ash by 18% and 12% for the N and R mixtures, respectively. These results suggest that this retarding effect

**Table 5—Results of compressive and tensile strengths**

| Mixtures | A | B | NF15 | NF22.5 | NF30 | RF15 | RF22.5 | RF30 |
|---|---|---|---|---|---|---|---|---|
| Compressive strength, MPa (psi × 10³) | | | | | | | | |
| 8 h | 15 (2.2) | 16 (2.3) | — | — | — | 10 (1.5) | 8 (1.2) | — |
| 1 day | 16 (2.3) | 18 (2.6) | 14 (2.0) | 13 (1.9) | 10 (1.5) | 20 (2.9) | 17 (2.5) | 13 (1.9) |
| 3 days | 21 (3.0) | 25 (3.6) | 24 (3.5) | 20 (2.9) | 18 (2.6) | 32 (4.6) | 30 (4.3) | 22 (3.1) |
| 7 days | 28 (4.1) | 35 (5.1) | 31 (4.5) | 30 (4.3) | 27 (3.9) | 38 (5.5) | 37 (5.3) | 31 (4.5) |
| 28 days | 34 (4.9) | 38 (5.5) | 41 (5.9) | 43 (6.2) | 36 (5.2) | 42 (6.1) | 41 (5.9) | 38 (5.5) |
| 56 days | 35 (5.1) | 43 (6.2) | 43 (6.2) | 45 (6.5) | 47 (6.8) | 44 (6.4) | 45 (6.5) | 42 (6.1) |
| Tensile strength, MPa (psi) | | | | | | | | |
| 1 day | 1.1 (160) | 1.8 (260) | 1.4 (205) | 1.3 (190) | 0.9 (130) | 2.1 (305) | 1.9 (275) | 1.2 (175) |
| 3 days | 1.9 (275) | 2.8 (405) | 2.6 (375) | 2.7 (390) | 1.9 (275) | 2.8 (405) | 2.8 (405) | 2.3 (335) |
| 7 days | 2.8 (405) | 3.1 (450) | 3.8 (550) | 3.7 (335) | 3.5 (505) | 3.8 (550) | 3.2 (465) | 2.7 (390) |
| 28 days | 3.2 (465) | 4.1 (595) | 5.1 (740) | 5.3 (770) | 5.7 (825) | 4.9 (710) | 5.2 (755) | 5.5 (800) |

was marginal, because it was discounted by the addition of nanosilica, which markedly sped up the kinetics of reactions, as discussed previously. Hence, the addition of nanosilica to the fly ash binders enhanced the hydration level and shortened the hardening time, which affects the early-age strength, as will be discussed in the next section.

## Strength

Table 5 shows the average compressive and splitting tensile strengths of specimens from all mixtures at different ages. The results generally indicated that the commercial products (A and B) gained the highest compressive strength at 8 hours; however, the increase in strength for these products was not significant until 1 day, while the RF15 and RF22.5 specimens achieved higher or comparable compressive strengths of 20 and 17 MPa (2900 and 2465 psi), respectively, at 1 day. In addition, the rate of strength development for products A and B was insignificant up to 3 days. This was statistically supported by the analysis of variance (ANOVA) at a significance level $\alpha = 0.05$.[28] For example, for Product A, ANOVA for the compressive results at 8 hours and 3 days had an $F$ value of 6.71, which is smaller than the critical value ($F_{cr}$) of 7.71. This insignificant change in compressive strength up to 3 days may be attributed to the very rapid reactions during the first 8 hours, which might have formed thick hydration shells that discounted the diffusion of water and kinetics of hydration afterward. Comparatively, the rate of strength development of the nano-modified mixtures was significant (an increase of 53 to 80%) up to 3 days. For instance, ANOVA for the compressive strength at 1 and 3 days for the NF15 and RF15 specimens yielded $F$ values of 28.6 and 33.7, respectively, which are larger than the corresponding $F_{cr}$ of 7.71. The results of the nano-modified mixtures at 28 and 56 days indicated that there was continuous and significant improvement in strength beyond 7 days in comparison to the commercial products. The significant increase in strength of these mixtures with time can be ascribed to the synergistic effects of nanosilica and fly ash, as will be discussed later in the TG results.

For specimens from the R mixtures, the average early-age (up to 7 days) strength significantly increased (15 to 43%) in comparison to the N mixtures. This is ascribed to the presence of the accelerating admixture, which sped up the rate of hydration reactions and consequently increased the early-age strength. However, this trend diminished between 7 to 56 days for the R mixtures, which conforms to effect of accelerators on the compressive strength development of concrete at later ages due to the slower diffusion of water through thicker hydration products.[22,23] Although increasing the dosage of fly ash in the mixtures led to reducing the compressive strength at early age, the N and R specimens with 30% fly ash (NF30 and RF30) had compressive strength values of 18 and 22 MPa (2610 and 3190 psi) at 3 days, respectively. For the NF30 mixture, the compressive development was significant after 7 days (70% increase between 7 to 56 days) and achieved the highest strength at 56 days (47 MPa [6817 psi]), which is consistent with the well-known effect of Class F fly ash on compressive strength of concrete.[6]

The early-age (1 to 7 days) results generally indicate that the compressive strength of the N and R nano-modified fly ash mixtures markedly improved with the addition of nanosilica, as no low values were observed for any mixture. These results are consistent with other studies.[8,10] Hence, the slow rate of strength development for concrete incorporating Class F fly ash can be controlled by the addition of a small dosage of nanosilica. It appears that nanosilica aggregates effectively contributed to the strength development of the mixtures up to 7 days through high pozzolanic activity,[11] filler effect,[29,30] and water absorption.[30] Moreover, nanosilica can catalyze the reactivity of fly ash at earlyage,[8] while the long-term improvement in strength of the mixtures can be ascribed to the continual pozzolanic effect of fly ash with time.[6] These mechanisms are discussed in detail later in the TG and microscopy analyses section.

The splitting tensile strength of concrete mixtures was determined at different ages, as listed in Table 5. The early-age tensile strength of product A was low, and this product had the lowest tensile strength at 28 days. Comparatively, product B gained higher tensile strength (1.8 MPa [261 psi]) at 1 day; in addition, the increase of tensile strength for product B was significant up to 28 days. Complying with the compressive strength results, all the nano-modified fly ash concrete
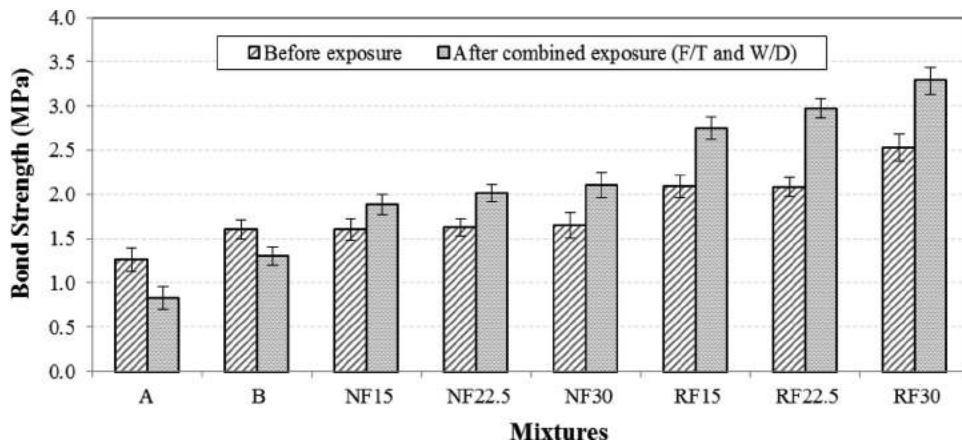
*Fig. 3—Bond strength of the repair assembly from pulloff test. (Note: 1 MPa = 145 psi; error bars in this figure represent standard error.)*

mixtures exhibited comparable or higher tensile strength up to 7 days (2.7 to 3.8 MPa [391 to 551 psi]) and 28 days (4.9 to 5.7 MPa [710 to 827 psi]) with a significant rate of increase. The effect of the accelerating admixture on the early-age results of tensile strength was similar to that of the compressive strength. Also, it was observed that the tensile strength slightly decreased with the fly ash content at early age; however, this trend was reversed at 28 days due to the continual reactivity of fly ash, as the N and R specimens with 30% fly ash had the highest tensile strength (Table 5). This behavior may be attributable to the densification of the interfacial transition zone (ITZ) between aggregate and cement paste as a result of the combined effects of nanosilica and fly ash, as shown later in the microscopy analysis section.

## Bonding

Bond failure is a critical cause of deterioration in pavement repairs. Therefore, the pulloff test was used to assess the bond strength of the repair mixtures with substrate concrete; this represents a severe scenario for the assembly, as it is subjected to a direct tension configuration. Also, the pulloff test was used to evaluate the residual bond strength of the mixtures to substrate concrete after combined cyclic environments, which should capture performance risks originating from incompatibility between the repair mixtures and substrate concrete. Therefore, a combined exposure protocol was adopted to replicate consecutive winter and summer seasons, which correlate to in-service conditions. Li et al.[31] used a similar technique to evaluate the bonding performance of rapid-setting repair materials subjected to F/T cycles.

The average bond strength values before and after the combined exposure are shown in Fig. 3. The average value of pulloff strength from specimens (four cores) produced a coefficient of variation of less than 20% (except for product A). The results showed that the commercial products A and B had bond strength of 1.3 and 1.6 MPa (188 and 232 psi), respectively. The bond strength of these products decreased significantly after the combined exposure by 48 and 31%, respectively, relative to the initial values. The failure of these specimens occurred mainly at the interface between the repair products and substrate concrete (reflecting some level

of incompatibility) or in the repair products due to their lower tensile capacity (Table 5). Comparatively, the bond strength for the N and R mixtures ranged between 1.9 to 3.3 MPa (275 to 478 psi), and it significantly increased by 23% to 43% after the combined exposure. In addition, the failure in specimens prepared with the N and R mixtures shifted toward the substrate concrete, suggesting that the assembly behaved as an integral system with a high degree of compatibility. Unlike the commercial products, the nano-modified fly ash system offset the deleterious debonding effects induced by cyclic environments and improved the later-age bonding with substrate concrete. This improvement in the bond strength after the combined exposure is thought to be attributed to the continual reactivity of the ternary binder with time of exposure, which might be facilitated by the enhanced moisture level in the repair concrete due to the use of a salt solution rather than fresh water.[32]

The evolution of the bond strength significantly increased (by 45% to 57%) for the R mixtures in comparison to corresponding specimens from the N mixtures. This may be ascribed to the presence of the accelerating admixture, which sped up the rate of hydration reactions and consequently improved the bond at the interface with substrate concrete since the early stage. In addition, increasing the dosage of fly ash led to increasing the bond strength notably, especially for the R mixtures, as depicted in Fig. 3. This improvement in bonding of the assembly might stem from the chemical interaction between nanosilica and fly ash with the available $Ca(OH)_2$ in the substrate concrete forming secondary calcium-silicate-hydrate (C-S-H) at the bond interface and, thus, enhancing the mechanical interlock between the two layers. The latter argument is substantiated by the efficient reactivity of binder and densified microstructure observed for mixtures comprising higher dosages of fly ash, as shown by the RCPT and thermal and microscopy tests.

## Penetrability

The penetrability of all repair mixtures was evaluated by the RCPT at 28 days, and the results of passing charges and physical penetration depth are listed in Table 6. The commercial product A had a high passing charge value, indicating coarse and continuous pore structure despite

achieving a compressive strength of 34 MPa (4930 psi) at this age. According to the classification of ASTM C1202,[20] all the nano-modified fly ash concrete mixtures had "very low" penetrability, as their passing charges were below 1000 coulombs, with comparable performance among the N and R mixtures incorporating similar dosages of fly ash. Correspondingly, these mixtures had markedly lower penetration depths (less than 10 mm [0.39 in.]) relative to that of the repair products A (50 mm [1.97 in.]) and B (15 mm [0.59 in.]).

The dosage of fly ash in the mixtures had a significant effect on the penetration depth. Considerable reduction of penetrability was achieved for the N and R mixtures containing 30% fly ash, which had comparable compressive strength to that of the commercial repair products at 28 days. ANOVA for the penetration depth results showed that increasing the fly ash content from 15% to 30% in the N and R mixtures had $F$ values 50.3 and 46.2, which are more than the critical value $F_{cr}$ of 4.1. This trend indicates the densification and discontinuity of the pore structure, which can be explained by the effects of nanosilica and fly ash, as shown later in the thermal and microscopy analyses section, thus improving the durability of the mixtures to the ingress of fluids and, in turn, their projected long-term performance.

**Table 6—Rapid chloride penetrability test (RCPT) results**

| Mixture ID | Passing charges, coulombs | Chloride ion penetrability class (ASTM C1202) | Average penetration depth, mm [standard error] |
|---|---|---|---|
| A | > 4000 | High | 50 [0] |
| B | 1443 | Low | 15 [1.0] |
| NF15 | 772 | Very low | 8 [0.4] |
| NF22.5 | 621 | Very low | 5 [0.7] |
| NF30 | 522 | Very low | 3 [0.3] |
| RF15 | 921 | Very low | 9 [0.7] |
| RF22.5 | 644 | Very low | 6 [0.7] |
| RF30 | 602 | Very low | 5 [0.4] |

Note: 1 mm = 0.0394 in.

## Surface scaling

The results of surface scaling due to the combined action of deicing salt and F/T cycles (ASTM C672)[19] are shown in Fig. 4 and 5. Product A showed a high tendency to surface scaling after approximately 10 cycles. After 50 cycles, products A and B had cumulative mass losses of 2.4 kg/m$^2$ (0.49 lb/ft$^2$) (visual rating of 4 to 5) and 0.5 kg/m$^2$ (0.10 lb/ft$^2$) (visual rating of 1 to 2), receptively. Bureau du normalization du Quebec (BNQ)[33] and the Ministry of Transportation, Ontario (MTO)[34] stipulate that the failure limits in salt-frost scaling tests are 0.50 and 0.80 kg/m$^2$ [0.10 and 0.16 lb/ft$^2$], respectively. According to these criteria, considering the difference in procedures among the three tests (for example, BNQ and MTO use a less aggressive solution of 3% sodium chloride), products A and B are deemed unacceptable, as they will likely have surface scaling issues in the field. In contrast, all the nano-modified concrete mixtures had limited surface scaling (maximum mass loss of 0.25 kg/m$^2$ [0.05 lb/ft$^2$] [Fig. 4]) and low visual ratings (0 to 1 [Fig. 5]), without a significant difference between the N and corresponding R mixtures. Minor popouts were observed, likely due to the deterioration of some porous aggregates near the surface of concrete.

It has been reported that the resistance to salt-frost scaling decreases with increasing the dosage of fly ash in concrete, which is among the key reasons that deter the wider use of higher dosages of fly ash in concrete pavements.[5-7] High contents of Class F fly ash in concrete may lead to significant proportions of unbound fly ash particles in the paste, resulting in coarse microstructure and higher tendency to surface scaling.[5-7] In the current study, incorporation of 30% fly ash in concrete led to a marginal increase in surface scaling as the binders were modified with nanosilica, indicating improved durability. This was shown by ANOVA for the results of surface scaling that showed a statistically insignificant difference between 15% and 30% fly ash in the N and R mixtures at 50 F/T cycles, as the $F$ values were 3.8 and 9.4, respectively, which are less than the $F_{cr}$ of 18.51. In addition, when the curing method and time were varied (Table 7), the mass loss results for Mixtures NF30 and RF30 were still below 0.5 kg/m$^2$ (0.10 lb/ft$^2$). The limited surface scaling of the concrete mixtures can be attributed to the incorporation of nanosilica with fly ash, which enhanced the reactivity and
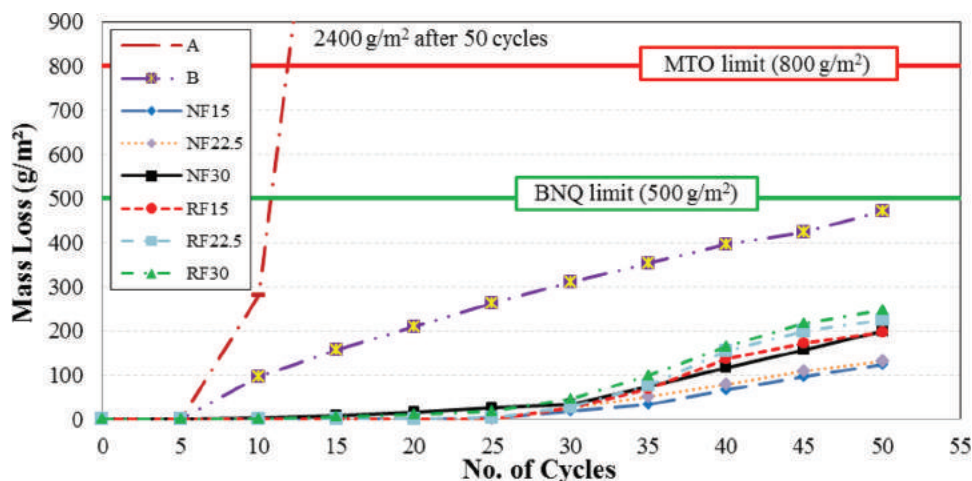


*Fig. 4—Mass loss of slabs tested according to ASTM C672. (Note: 1 g/m$^2$ = 2.05 × 10$^{-4}$ lb/ft$^2$.)*

**Table 7—Effect of curing time and method on average mass loss results after 50 freezing-and-thawing cycles**

| Curing method | Mass loss, g/m$^2$ | | | | | |
|---|---|---|---|---|---|---|
| | NF15 | NF22.5 | NF30 | RF15 | RF22.5 | RF30 |
| 14 days curing* and 14 days in air (ASTM C672) | 123 | 132 | 189 | 196 | 226 | 247 |
| 3 days curing* and 14 days in air | 147 | 229 | 398 | 152 | 248 | 410 |
| Curing* the concrete until strength of 20 MPa and 14 days in air | 142 | 221 | 331 | 210 | 363 | 489 |
| Curing by a chemical compound† and 14 days in air | 163 | 177 | 236 | 241 | 274 | 376 |

*Maintained at a temperature of 23 ± 2°C (73.4 ± 35.6°F) and relative humidity of more than 95%.

†Curing compound met CSA A23.1-14 (Clause 7.7.2.2) specifications.

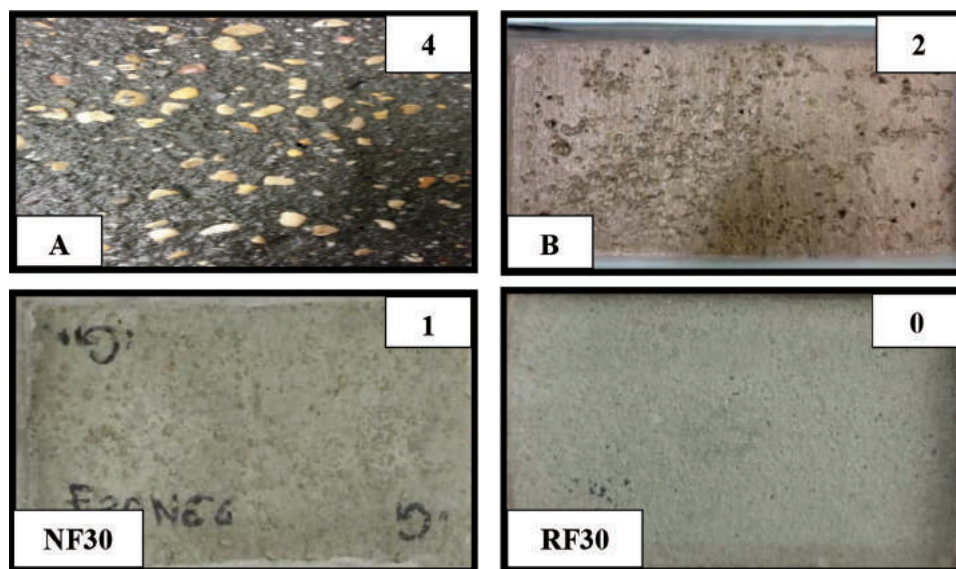Note: 1 g/m$^2$ = 2.05 × 10$^{-4}$ lb/ft$^2$.



*Fig. 5—Exemplar visual ratings of slabs after 50 freezing-and-thawing cycles.*

binding of Class F fly ash, as indicated, for example, by the evolution of compressive and tensile strengths. According to the glue-spall theory,[35] which employs fracture mechanics to explain the process of salt-frost scaling by crack propagation into the surface of concrete, the strength of cementitious matrix substantially controls its resistance to scaling. The combination of fly ash with nanosilica led to a dense matrix/ITZ (further densifying with time) and higher tensile capacity, as shown by various tests (for example, bonding, RCPT, BSEM), which might discount the process of crack propagation in the surface of concrete and, thus, improve its resistance to salt-frost scaling.

**Thermal and microscopy analyses**

The consumption of portlandite (CH) in the cementitious matrix was determined at different ages to capture the evolution of hydration and pozzolanic reactions, as shown in Fig. 6. At a constant dosage of nanosilica (6%), consumption of CH in the N and R mixtures started at a very early age. For example, at 1 day, the normalized CH contents for NF15 and NF30 relative to the corresponding reference mixtures were less than 1.0 (Fig. 6), which may be linked to a vigorous pozzolanic activity at early age, as observed in the heat of hydration (Fig. 2) and strength tests (Table 5). It has been

postulated that a very rapid pozzolanic activity is possible as silicate ions from nanosilica aggregates engage with CH forming pozzolanic C-S-H gel, which subsequently precipitate on the surface of silica aggregates, resulting in slower reactivity at later ages.[9,27,30] Whether this mechanism is a through-solution process[9] or topochemical growth[30] is still debatable. Moreover, nanosilica can accelerate the hydration of cement by creating additional surfaces for early precipitation of hydration products.[9,11,27] Also, It has been shown that commercial nanosilica sols (originally dispersed to their primary sizes) form small-enough agglomerates to impart a filler effect in the cementitious matrix.[29,30] All these factors might have contributed to improving the early-age strength (up to 7 days) of nano-modified fly ash concrete, even for mixtures incorporating 30% fly ash (Table 5).

It has been documented that the pozzolanic effect of fly ash in concrete starts at later ages[5,22,23] (typically after 28 days; F15 and F30 in Fig. 6); therefore, most standard codes for concrete (for example, CSA A23.1 2014)[36] require the properties of fly ash concrete to be assessed at 56 or 91 days. It was reported[11] that the pozzolanic action of nanosilica aggregates is completed within 7 days; however, Fig. 6 shows a significant consumption in CH in the N and R mixtures from 7 to 90 days relative to the reference mixtures, especially at
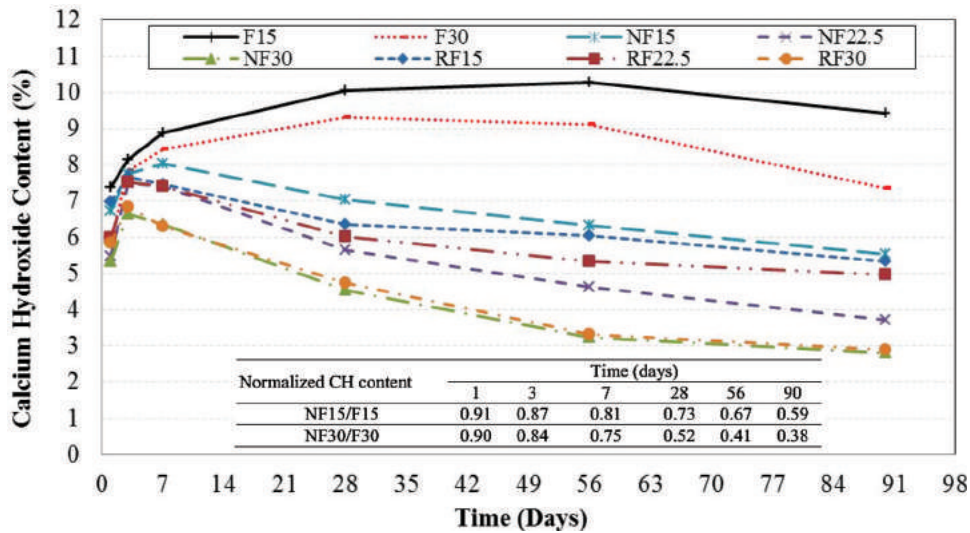
Fig. 6—Thermogravimetry results for the portlandite content (at a temperature range of 400 to 450°C [752 to 842°F]) in the nano-modified fly ash concrete mixtures.
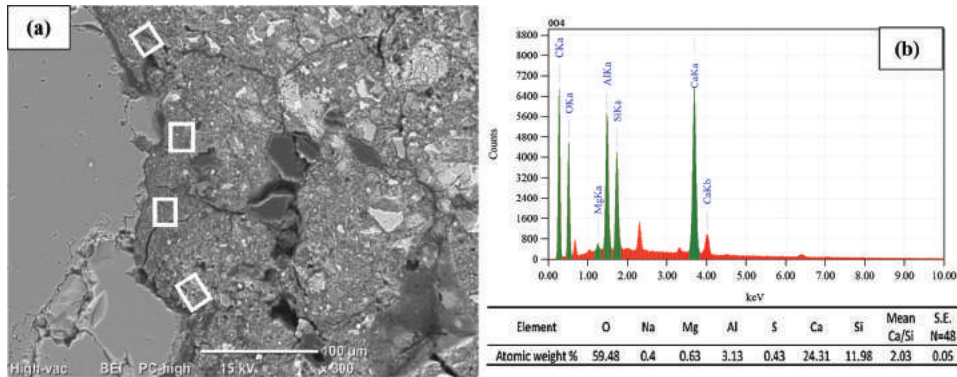


Fig. 7—BSEM analysis for a thin section from product A, showing: (a) porous ITZ and coarse microstructure; and (b) associated EDX spectrum of C-S-H in locations indicated in (a). (Note: S.E. is standard error.)

higher dosages of fly ash (NF30 and RF30). This pinpoints that the presence of nanosilica catalyzed the reactivity of fly ash in concrete, resulting in an improved level of hydration and an evolution of microstructure. The continual reactivity of the ternary binder up to 90 days is attributed to the pozzolanic activity of fly ash with time, as, for example, noted in the results of later-age strength (Table 5) and bonding after the combined exposure (Fig. 3). This explains the significant densification and refinement of the pore structure at 28 days in the nano-modified fly ash concrete mixtures, which had limited penetration depth (average of 6 mm [0.24 in.]).

BSEM was conducted on thin sections to complement the trends observed in the mechanical, durability, and TG tests. In comparison to the commercial product A, all the nano-modified fly ash mixtures had a significant degree of refinement and densification in the hydrated paste and ITZ at 28 days. Product A (Fig. 7) showed coarse microstructure in addition to microcracks in the paste and ITZ; the EDX analysis for C-S-H in the ITZ showed a high calcium-silicate ratio (*C/S*) (average of 2.0). These features reflect an insufficient level of hydration conforming to the inferior performance observed for this product in the mechanical and durability tests. On the contrary, homogenous and dense matrix in various specimens from the N and R mixtures with low (15%) and high

(30%) dosages of fly ash were observed. For instance, Fig. 8 shows dense microstructure and refined ITZ at 28 days of a specimen from NF30 owing to the synergistic effects of nanosilica and fly ash, as described previously. EDX analysis for C-S-H in the ITZ in this specimen showed that the average *C/S* was 1.05, indicating an efficient pozzolanic activity, and densification of ITZ with secondary C-S-H. It was reported that the *C/S* of secondary C-S-H from pozzolanic reactions is lower than that of conventional C-S-H produced from cement hydration reactions, the former has a ratio of approximately 1.1, whereas the latter has a ratio of approximately 1.7.[37] In addition, Kong et al.[30] stated that when small agglomerates of nanosilica form, water absorption into their ultra-high nano-porosity can reduce the water-binder ratio (*w/b*) in the paste, thus improving the microstructure of the matrix.

## CONCLUSIONS

Considering the materials, mixture designs, and testing methods implemented in this study, the following conclusions can be drawn:

1. This study indicates that the high early-strength of rapid-setting materials is an insufficient criterion to consider a product acceptable as a repair material for concrete pave-
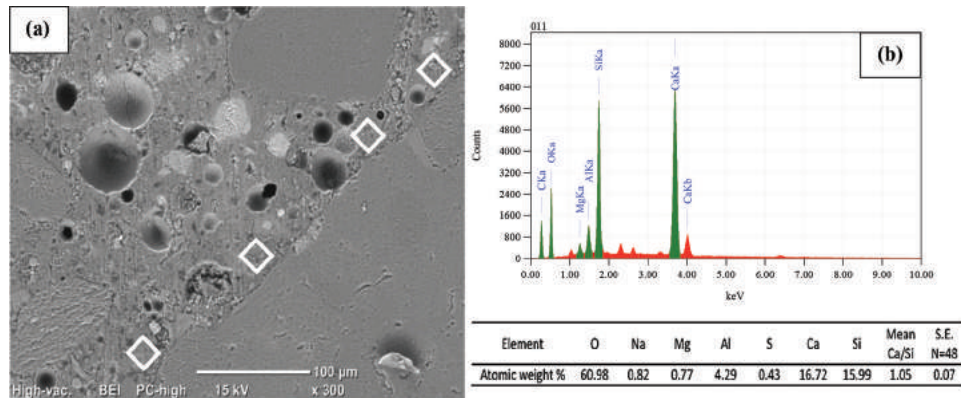
*Fig. 8—BSEM analysis for a thin section from NF30, showing: (a) refined ITZ and dense microstructure; and (b) associated EDX spectrum of C-S-H in the locations indicated in (a). (Note: S.E. is standard error.)*

ments. Except for early-age strength, the commercial product A had adverse performance in many aspects such as placement/finishability and salt-frost scaling. Comparatively, product B had better performance in early-age strength and resistance to the ingress of fluids and salt-frost scaling.

2. The normal and rapid nano-modified fly ash concrete mixtures developed herein had ample hardening times, without excessive delay, which improves the flexibility and quality of the repair process with suitability for different repair applications (for example, multiple/large patch areas with less critical opening time to traffic).

3. The incorporation of 6% nanosilica in concrete with up to 30% fly ash significantly shortened the dormant period and accelerated the rate of hydration reactions, which discounted some of the retarding effect of Class F fly ash on the rate of hardening of concrete.

4. The synergistic effects of nanosilica and fly ash in both the N and R mixtures improved the early-age and long-term compressive, tensile, and bond (even after the combined exposure) strengths of concrete, which indicate that the inherently slower rate of strength and microstructural development of concrete containing Class F fly ash can be controlled by the addition of small dosages of nanosilica.

5. The combination of fly ash with nanosilica led to a dense pore structure (as shown by the low penetration depth in the RCPT) and improved tensile capacity (as reflected by the limited surface scaling of concrete), which suggest that the addition of nanosilica with fly ash enhanced its binding in the matrix.

6. In addition to the effects of nanosilica on improving the hydration and pore structure characteristics by multiple mechanisms, TG results showed that addition of 6% nanosilica to concrete incorporating up to 30% fly ash catalyzed the reactivity of Class F fly ash, resulting in an improved level of hydration and an evolution of microstructure with age. This explains the significant densification/refinement in the hydrated paste and ITZ, as shown by BSEM at 28 days, and the corresponding improved mechanical and durability performance of the nano-modified fly ash concrete at different ages.

The overall results indicate that nano-modified fly ash concrete can achieve balanced early-age and long-term performance. Hence, it presents a viable option for a suite of repair applications in concrete pavements, with an anticipated measurable impact on reducing life cycle costs. Yet, its field performance needs to be documented, which is recommended for future work.

## AUTHOR BIOS
*ACI member* **A. Ghazy** *is a PhD Candidate at the University of Manitoba, Winnipeg, MB, Canada. He received his BSc and MSc from Alexandria University, Egypt. His research interests include durability of concrete pavements.*

*ACI member* **M. T. Bassuoni** *is an Associate Professor in the Department of Civil Engineering at the University of Manitoba. He is a member of ACI Committees 201, Durability of Concrete; 236, Material Science of Concrete; 237, Self-Consolidating Concrete; and 241, Nanotechnology of Concrete. His research interests include cementitious materials and durability of concrete.*

**A. Shalaby** *is a Professor in the Department of Civil Engineering at the University of Manitoba. His research interests include pavement engineering and infrastructure management.*

## REFERENCES
1. Al-Ostaz, A.; Irshidat, M.; Tenkhoff, B.; and Ponnapalli, P. S., "Deterioration of Bond Integrity between Repair Material and Concrete due to Thermal and Mechanical Incompatibilities," *Journal of Materials in Civil Engineering*, ASCE, V. 22, No. 2, 2010, pp. 136-144. doi: 10.1061/(ASCE)0899-1561(2010)22:2(136)

2. Li, M., and Victor, C. L., "High-Early-Strength Engineered Cementitious Composites for Fast, Durable Concrete Repair-Material," *ACI Materials Journal*, V. 108, No. 1, Jan.-Feb. 2011, pp. 3-12.

3. Soliman, H., and Shalaby, A., "Characterizing The Performance of Cementitious Partial-Depth Repair Materials in Cold Climates," *Construction & Building Materials*, V. 70, 2014, pp. 148-157. doi: 10.1016/j.conbuildmat.2014.07.114

4. Bentz, D. P., and Peltz, M. A., "Reducing Thermal and Autogeneous Shrinkage Contributions to Early-Age Cracking," *ACI Materials Journal*, V. 105, No. 4, July-Aug. 2008, pp. 414-420.

5. Malhotra, V. M.; Zhang, M. H.; Read, P. H.; and Ryell, J., "Long-Term Mechanical Properties and Durability Characteristics of High-Strength/High-Performance Concrete Incorporating Supplementary Cementing Materials Under Outdoor Exposure Conditions," *ACI Materials Journal*, V. 97, No. 5, Sept.-Oct. 2000, pp. 518-525.

6. Ondova, M.; Stevulova, N.; and Meciarova, L., "The Potential of Higher Share of Fly Ash Cement Replacement in the Concrete Pave-

ment," *Procedia Engineering*, V. 65, 2013, pp. 45-50. doi: 10.1016/j.proeng.2013.09.009

7. Huang, C.; Lin, S.; Chang, C.; and Chen, H., "Mix Proportions and Mechanical Properties of Concrete Containing Very High-Volume of Class F fly ash," *Construction & Building Materials*, V. 46, 2013, pp. 71-78. doi: 10.1016/j.conbuildmat.2013.04.016

8. Said, A. M.; Zeidan, M. S.; Bassuoni, M. T.; and Tian, Y., "Properties of Concrete Incorporating Nano-silica," *Construction & Building Materials*, V. 36, 2012, pp. 838-844. doi: 10.1016/j.conbuildmat.2012.06.044

9. Madani, H.; Bagheri, A.; and Parhizkar, T., "The Pozzolanic Reactivity of Monodispersed Nanosilica Hydrosols and Their Influence on the Hydration Characteristics of Portland Cement," *Cement and Concrete Research*, V. 42, No. 12, 2012, pp. 1563-1570. doi: 10.1016/j.cemconres.2012.09.004

10. Belkowitz, J. S.; Belkowitz, W. L. B.; Nawrocki, K.; and Fisher, F. T., "Impact of Nanosilica Size and Surface Area on Concrete Properties," *ACI Materials Journal*, V. 112, No. 3, May-June 2015, pp. 419-428. doi: 10.14359/51687397

11. Hou, P.; Kawashima, S.; Kong, D.; Corr, D.; Qian, J.; and Shah, S., "Modification Effects of Colloidal NanoSiO$_2$ on Cement Hydration and its Gel Property," *Composites. Part B, Engineering*, V. 45, No. 1, 2013, pp. 440-448. doi: 10.1016/j.compositesb.2012.05.056

12. CAN/CSA-A3001, "Cementitious Materials for Use in Concrete," Canadian Standards Association, Mississauga, ON, Canada, 2008.

13. ASTM C494/C494M-13, "Standard Specification for Chemical Admixtures for Concrete," ASTM International, West Conshohocken, PA, 2013, 10 pp.

14. ASTM C403/C403M-08, "Standard Test Method for Time of Setting of Concrete Mixtures by Penetration Resistance," ASTM International, West Conshohocken, PA, 2008, 7 pp.

15. ASTM C1679-14, "Standard Practice for Measuring Hydration Kinetics of Hydraulic Cementitious Mixtures Using Isothermal Calorimetry," ASTM International, West Conshohocken, PA, 2014, 7 pp.

16. ASTM C39/C39M-12, "Standard Test Method for Compressive Strength of Cylindrical Concrete Specimens," ASTM International, West Conshohocken, PA, 2012, 7 pp.

17. ASTM C496/C496M-11, "Standard Test Method for Splitting Tensile Strength of Cylindrical Concrete Specimens," ASTM International, West Conshohocken, PA, 2011, 5 pp.

18. CSA A23.2-6B, "Determination of Bond Strength of Bonded Toppings and Overlays and of Direct Tensile Strength of Concrete, Mortar, and Grout," CSA A23.1/A23.2, Canadian Standards Association, Mississauga, ON, Canada, 2014.

19. ASTM C672/C672M-14, "Standard Test Method for Scaling Resistance of Concrete Surfaces Exposed to De-icing Chemicals," ASTM International, West Conshohocken, PA, 2014, 3 p.

20. ASTM C1202-12, "Standard Test Method for Electrical Indication of Concrete's Ability to Resist Chloride Ion Penetration," ASTM International, West Conshohocken, PA, 2012, 8 p.

21. Bassuoni, M. T.; Nehdi, M.; and Greenough, T., "Enhancing the Reliability of Evaluating Chloride Ingress in Concrete Using the ASTM C 1202 Rapid Chloride Penetrability Test," *Journal of ASTM International*, V. 3, No. 3, 2006, 13 p.

22. Nevile, A. M., Properties of Concrete, Prentice Hall, London, UK, 2011, 983 pp.

23. Mehta, P. K., and Monteiro, P. J. M., *Concrete*, McGraw Hill Education, 2014, 675 pp.

24. Stein, H. N., and Stevels, J. M., "Influence of Silica on the Hydration of 3CaO, SiO$_2$," *Journal of Application Chemistry*, V. 14, No. 8, 1964, pp. 338-346. doi: 10.1002/jctb.5010140805

25. Depasse, J., "Simple Experiments to Emphasize the Main Characteristics of the Coagulation of Silica Hydrosols by Alkaline Cations: Application to the Analysis of the Model of Colic et al," *Journal of Colloid and Interface Science*, V. 220, No. 1, 1999, pp. 174-176. doi: 10.1006/jcis.1999.6594

26. Zerrouk, R.; Foissy, A.; Mercier, R.; Chevallier, Y.; and Morawski, J. C., "Study of Ca$^{2+}$ Induced Silica Coagulation by Small Angle Scattering," *Journal of Colloid and Interface Science*, V. 139, No. 1, 1990, pp. 20-29. doi: 10.1016/0021-9797(90)90441-P

27. Korpa, A.; Kowald, T.; and Trettin, R., "Hydration Behaviors, Structure and Morphology of Hydration Phases in Advanced Cement-Based Systems Containing Micro and Nanoscale Pozzolanic Additives," *Cement and Concrete Research*, V. 38, No. 7, 2008, pp. 955-962. doi: 10.1016/j.cemconres.2008.02.010

28. Montgomery, D. C., *Design and Analysis of Experiments*, John Wiley and Sons, New York, 2014, 326 pp.

29. Oertel, T.; Hutter, F.; Tanzer, R.; Helbig, U.; and Sextl, G., "Primary Particle Size and Agglomerate Size Effects of Amorphous silica in Ultra-High Performance Concrete," *Cement and Concrete Composites*, V. 37, 2013, pp. 61-67. doi: 10.1016/j.cemconcomp.2012.12.005

30. Kong, D.; Du, X.; Wei, S.; Zhang, H.; Yang, Y.; and Shah, S. P., "Influence of Nano-Silica Agglomeration on Microstructure and Properties of the Hardened Cement-Based Materials," *Construction & Building Materials*, V. 37, 2012, pp. 707-715. doi: 10.1016/j.conbuildmat.2012.08.006

31. Li, S.; Frantz, G. C.; and Stephens, J. E., "Bond Performance of Rapid-Setting Repair Materials Subjected to De-icing Salt and Freezing-Thawing Cycles," *ACI Materials Journal*, V. 96, No. 6, Nov.-Dec. 1999, pp. 692-697.

32. Spragg, R. P.; Castro, J.; Li, W.; Pour-Ghaz, M.; Huang, P.; and Weiss, J., "Wetting and Drying of Concrete Using Aqueous Solutions Containing Deicing Salts," *Cement and Concrete Composites*, V. 33, No. 5, 2011, pp. 535-542. doi: 10.1016/j.cemconcomp.2011.02.009

33. BNQ NQ 2621-900, "Determination of the Scaling Resistance of Concrete Surfaces Exposed to Freezing-and-Thawing Cycles in the Presence of De-icing Chemicals," Bureau de Normalisation du Québec, Annexe A, 2002, pp. 19-22.

34. MTO LS-412, "Method of Test For Scaling Resistance of Concrete Surfaces Exposed to Deicing Chemicals," *Ontario Lab Testing Manual*, Ministry of Transportation, 1997.

35. Valenza, J. J. II, and Scherer, G. W., "A Review of Salt Scaling: II. Mechanisms," *Cement and Concrete Research*, V. 37, No. 7, 2007, pp. 1022-1034. doi: 10.1016/j.cemconres.2007.03.003

36. CSA A23.1/A23.2, "Concrete Materials/Methods of Test and Standard Practices for Concrete," Canadian Standards Association, Mississauga, ON, Canada, 2014.

37. Detwiler, R.; Bhatty, J.; and Bhattacharja, S., "Supplementary Cementing Materials for use in Blended Cements," Portland Cement Association, Skokie, IL, 1996, 103 pp.